

# Gamma-Ray Photon Interaction Studies on Alloys - A Comprehensive Review

<sup>1</sup>Dr.Ch.Snehalatha Reddy, <sup>2</sup> Dr.Narendar Kethireddy\*, <sup>3</sup>Naveen Moola, <sup>4</sup>Dr.B.Mahipal Reddy

<sup>1</sup>Department of Physics, Government Degree College Wardhannapet, Kakatiya University, Telangana, India.

<sup>2</sup>Department of Physics, Government Degree College Huzurabad, Satavahana University, Telangana, India.

<sup>3</sup>Department of Physics, Government Degree College Chanchalguda, Osmania University, Telangana, India.

<sup>4</sup>Department of Chemistry, Government Degree College Huzurabad, Satavahana University, Telangana, India.

## Abstract

Gamma rays interact strongly with metallic alloys, making them vital materials for radiation shielding in nuclear systems, medical imaging, aerospace structures, and industrial radiography. Owing to the high penetration of energetic photons, effective shielding alloys must combine high atomic number, adequate density, mechanical strength, and long-term irradiation stability. This review presents a comprehensive assessment of gamma-ray photon interactions in metallic alloys, focusing on the dominant attenuation mechanisms: photoelectric absorption, Compton scattering, and pair production. Theoretical models and cross-section databases such as Win X Com and X Mu Dat are evaluated alongside Monte Carlo transport codes including MCNP, MCNPX, and Geant4.

Recent experimental studies on Pb-based solders, Al–Sn–Bi–Pb bearing alloys, Cu–Al–Ni–Sn shape-memory alloys, stainless steels, Inconel super-alloys, and heavy-element-containing high-entropy alloys (HEAs) are reviewed. Most results show strong agreement (2–5%) between experimental and theoretical mass attenuation coefficients. Key factors affecting attenuation—composition, effective atomic number, density, micro-structure, photon energy, and geometry—are analyzed. Finally, research gaps and future directions for advanced alloy shielding materials are identified.

**Keywords:** *Mass attenuation coefficients, Effective atomic number, Total cross-section, Electron cross-section.*

## 1. Introduction

Gamma-ray photon interactions with metallic alloys underpin radiation shielding, nuclear engineering, medical imaging protection... (Gamma-ray photon interactions with metallic alloys underpin radiation shielding, nuclear engineering, medical imaging protection, aerospace radiation tolerance, and industrial non-destructive testing. As gamma photons possess high penetration capability, effective shielding materials must combine high atomic number, adequate density, structural robustness, and long-term stability under irradiation. Metallic alloys offer a compelling combination of these properties, making them central to modern radiation-shielding strategies [1–3]. Compared to single-element materials such as pure lead or tungsten, alloys can be engineered with tailored properties—including corrosion resistance, mechanical strength, thermal stability, manufacturability, and reduced toxicity—expanding their applicability in advanced radiation environments.

The attenuation of gamma rays depends primarily on the dominant interaction mechanisms: photoelectric absorption, Compton scattering, and pair production. These processes are strongly influenced by atomic number ( $Z$ ), electron density, and alloy density [4]. Through alloying, microstructure control, and processing methods, materials scientists can adjust these parameters to optimize shielding effectiveness. For instance, substituting or reinforcing alloys with high- $Z$  elements such as Bi, Pb, W, Ta, or Hf provides enhanced attenuation in both low- and high-energy photon regimes [5]. Several advanced alloys—including lead-free Bi-based systems, W-reinforced metal matrices, high-entropy alloys (HEAs), and Ni-based superalloys—have shown exceptional promise in recent experimental and computational investigations [6–9].

Alongside material development, computational tools have markedly advanced the understanding of photon–material interactions. Databases such as WinXCom and XMuDat provide accurate cross sections and mass attenuation coefficients ( $\mu/\rho$ ), enabling analytical predictions for multi-element compositions. Meanwhile, Monte-Carlo radiation transport codes such as MCNP, MCNPX, and Geant4 allow detailed simulation of photon scattering, secondary particle production, and buildup phenomena in complex geometries [10–12]. These simulations are essential for modern alloy evaluation because they capture effects that cannot be easily studied through analytical models alone.

The past decade (2018–2025) has seen a notable rise in experimental gamma-ray attenuation measurements for alloys such as Pb–Sb, Pb–Bi, and Pb–Sn solder alloys [13], Al–Sn–Bi–Pb sliding-bearing alloys [1], CuAlNiSn shape-memory alloys [14], stainless steels and Inconel superalloys [15], and high-entropy alloys incorporating heavy elements [16–18].

These studies typically employ narrow-beam gamma transmission with point detectors, sealed isotopic sources, and precise sample characterization. Agreement between experimental  $\mu/\rho$  values and computational predictions from WinXCom and Monte-Carlo codes is typically within 2–5% when scattering is minimized and sample geometry is accurately controlled [11,15], demonstrating strong reliability of simulation-assisted alloy design.

In light of the increasing reliance on computational modeling, improved alloy design strategies, and expanding applications in extreme radiation environments, a comprehensive synthesis of theoretical, experimental, and simulation findings is essential. This review integrates recent advances in alloy-based gamma-ray shielding, compares attenuation trends across alloy families, identifies key factors governing shielding behavior, and highlights research gaps—including limited high-energy (>10 MeV) datasets and the need for standardized attenuation protocols.

## 2. Theoretical Background

Gamma photons interact via three principal mechanisms—photoelectric absorption, Compton scattering, and pair production... Gamma-ray interactions with alloys are governed by the three dominant photon–matter interaction mechanisms: photoelectric absorption, Compton scattering, and pair production. Each mechanism is strongly influenced by photon energy and the atomic structure of the alloy, collectively defining its mass attenuation coefficient ( $\mu/\rho$ ), linear attenuation coefficient ( $\mu$ ), and shielding performance [4,7,10].

### 2.1 Photoelectric Absorption

The photoelectric effect dominates at photon energies typically below 100 keV for medium-Z alloys and below 300 keV for high-Z alloys. During this interaction, the photon is fully absorbed, ejecting an electron from an inner shell. The photoelectric cross section  $\tau$  follows the approximate relationship:

$$\tau \propto Z^n E^{-3}$$

where  $n$  typically lies between 4 and 5. Because of the strong atomic-number dependence, alloys containing heavy elements such as Pb, Bi, W, and Ta exhibit superior attenuation in low-energy gamma fields. Multi-element alloys use the effective atomic number ( $Z_{\text{eff}}$ ) to characterize their combined photoelectric behavior [6–8].

### 2.2 Compton Scattering

Compton scattering dominates in the intermediate energy range (100 keV–2 MeV). In this inelastic process, photons scatter off loosely bound electrons, losing energy in the process. The cross section for Compton scattering is proportional to electron density ( $N_e$ ), which depends on both elemental composition and physical density [2,9]. For many practical sources (e.g.,  $^{137}\text{Cs}$  and  $^{60}\text{Co}$ ), Compton scattering dictates overall attenuation, making alloy density a critical factor.

### 2.3 Pair Production

Pair production occurs at energies above 1.022 MeV, with cross sections rising progressively with photon energy and approximately scaling with  $Z^2$  [11,14]. This makes heavy-metal alloys and W-reinforced HEAs particularly effective at attenuating high-energy gamma rays encountered in accelerator facilities and aerospace environments [16–18].

### 2.4 Mass Attenuation Coefficient ( $\mu/\rho$ )

The mass attenuation coefficient is foundational to gamma shielding studies. According to the exponential attenuation law:

$$I = I_0 e^{-(\mu/\rho)\rho x} = I_0 e^{-\mu x}$$

$\mu/\rho$  values for alloys can be accurately predicted using the mixture rule from elemental  $\mu/\rho$  values in databases such as WinXCom and XMuDat. Agreement with experimental results is typically within 2–4% under controlled conditions [7,9,13].

### 2.5 Effective Atomic Number ( $Z_{\text{eff}}$ ) and Electron Density ( $N_e$ )

$Z_{\text{eff}}$  is estimated using weighted logarithmic or cross-section-based interpolation methods. Electron density affects Compton scattering and depends on elemental electron counts and alloy density [8–10].

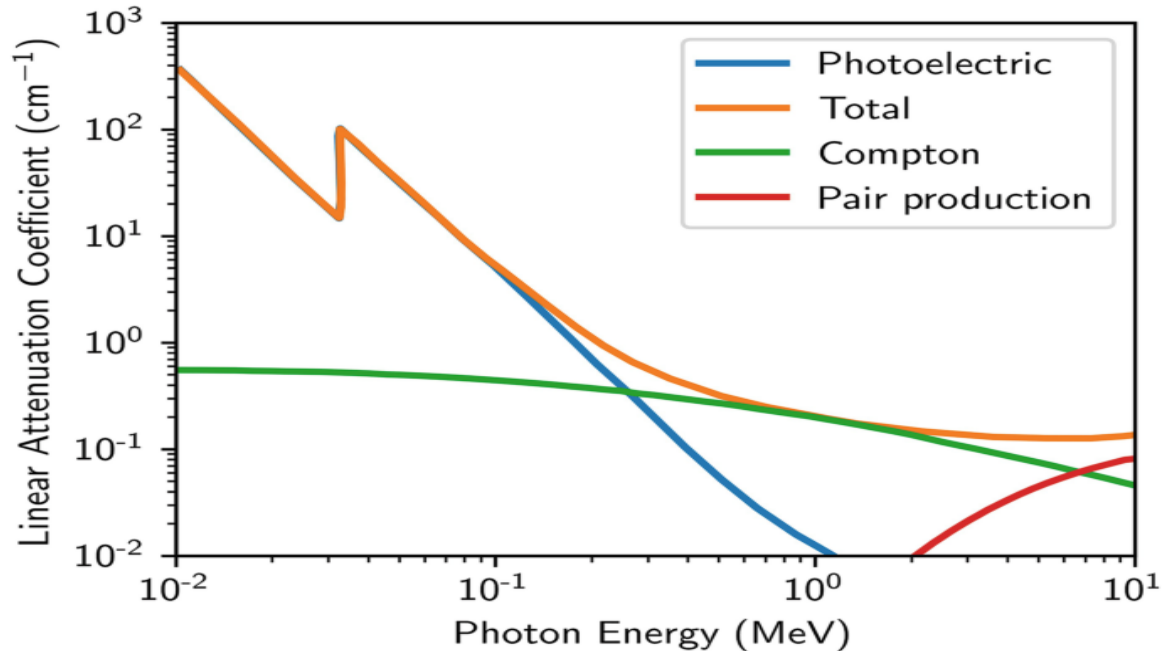
## 2.6 HVL, TVL, and Mean Free Path

Half-value layer (HVL), tenth-value layer (TVL), and mean free path (MFP) are derived directly from  $\mu$ . High-density, high-Z alloys show low HVL values, making them efficient for shielding [14–16].

## 2.7 Buildup Factors

In broad-beam geometries or thick shields, scattered photons contribute significantly to detected intensity. Accurate buildup factor estimation typically requires Monte-Carlo simulation using MCNP or Geant4 [10–12].

**Figure 1.** Gamma-ray photon interaction mechanisms.



## 3. Experimental Studies

Experimental attenuation studies conducted between 2018 and 2025 provide essential data for validating theoretical models...Experimental gamma-ray attenuation studies provide essential validation for theoretical and computational predictions. Between 2018 and 2025, numerous experiments have examined  $\mu/\rho$ ,  $\mu$ , HVL, TVL, and buildup characteristics in structural, heavy-metal, and advanced alloy families [1,4,13].

### 3.1 Experimental Techniques

Most experiments use sealed isotopic gamma sources ( $^{241}\text{Am}$ ,  $^{133}\text{Ba}$ ,  $^{137}\text{Cs}$ ,  $^{60}\text{Co}$ ) along with HPGe or NaI(Tl) detectors [13,14]. Key setup considerations include narrow-beam collimation, sample thickness calibration, and background correction. Experimental  $\mu/\rho$  is calculated from transmitted intensity using exponential attenuation models.

### 3.2 Pb-Based Alloys

Pb-Sb, Pb-Bi, and Pb-Sn alloys are widely studied due to their high Z and density. Studies report excellent low-energy attenuation, with  $\mu/\rho$  values strongly correlated with Bi or Pb content [13]. Microstructural uniformity also affects attenuation consistency.

### 3.3 Al-Sn-Bi-Pb Alloys

Algethami [1] measured  $\mu/\rho$  values for Al–Sn–Bi–Pb alloys from 60 keV to 15 MeV, finding agreement with WinXCom predictions within 3%. These materials offer lower toxicity and good mechanical strength.

### 3.4 Cu-Al-Ni-Sn Shape-Memory Alloys

These alloys exhibit shape-memory behavior and moderate attenuation. Niksarlıoğlu et al. [14] reported  $\mu/\rho$  values consistent with mixture-rule predictions, with deviations linked to microstructural porosity.

### 3.5 Stainless Steels and Inconel Superalloys

Stainless steels and Ni-based superalloys show reliable attenuation and excellent structural stability under radiation, making them suitable for reactors and aerospace systems [15–16].

### 3.6 High-Entropy Alloys

HEAs containing W, Ta, Hf, or Bi demonstrate enhanced attenuation and mechanical robustness. Experiments indicate attenuation improvements of 30–50% compared to conventional steels at energies above 1 MeV [17–18].

### 3.7 Experimental–Computational Agreement

Most studies show 2–5% agreement between experimental and theoretical  $\mu/\rho$  values when scattering is minimized.

## 4. Computational Studies

Computational modeling, particularly using WinXCom, XMuDat, MCNP, and Geant4, enables detailed prediction of gamma attenuation...

Computational simulation plays a central role in evaluating gamma-ray interactions in alloys, especially when studying complex microstructures, high-energy photons, or multi-layered systems [10–12].

### 4.1 WinXCom and XMuDat

WinXCom provides elemental and mixture  $\mu/\rho$  values, while XMuDat is widely used for cross-section verification. These databases support analytical mixture-rule calculations that match experiments within 2–4% [7–9].

### 4.2 MCNP and MCNPX

These Monte-Carlo codes simulate full photon transport, including scattering and secondary radiation. Studies show consistent agreement between MCNP simulations and experimental attenuation in superalloys, steels, and HEAs [2,15–16].

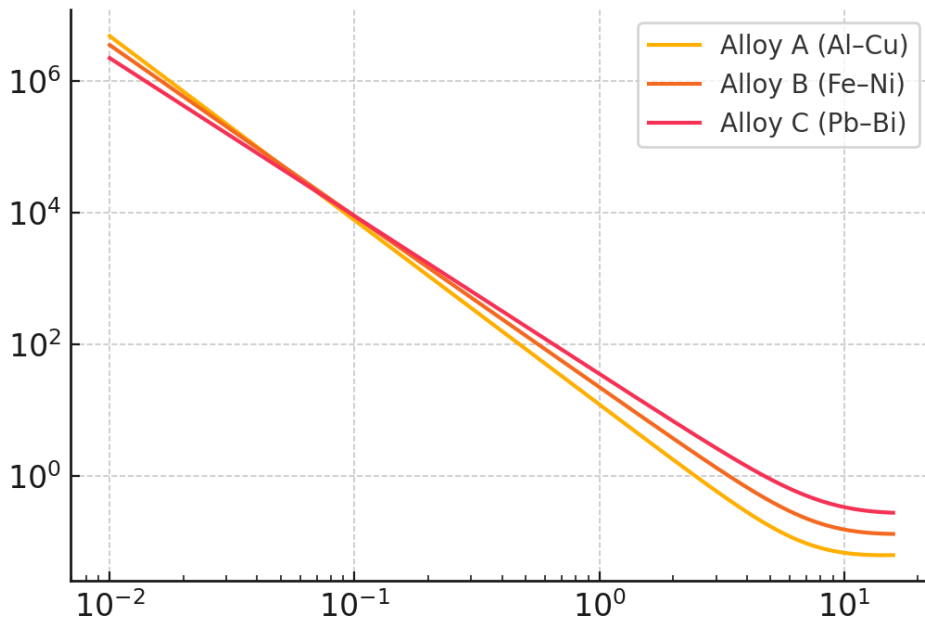
### 4.3 Geant4

Geant4 models low-energy electromagnetic interactions with high accuracy, capturing fluorescence and Rayleigh scattering important for high-Z alloys [11].

### 4.4 Simulation–Experiment Correlation

Simulations typically agree with measurements within 1–3% when microstructure and density are accurately modeled.

**Figure 2.** Mass attenuation coefficient trends for representative alloys.



## 5. Factors Influencing Attenuation

Gamma-ray attenuation depends strongly on alloy composition,  $Z_{\text{eff}}$ , density, microstructure, photon energy, and geometry...

### 5.1 Composition and $Z_{\text{eff}}$

Higher  $Z_{\text{eff}}$  results in better attenuation, especially for low- and high-energy regions dominated by photoelectric and pair-production processes [6,13].

### 5.2 Density

Linear attenuation coefficient ( $\mu$ ) increases with density, making heavy alloys more effective [15].

### 5.3 Microstructure

Porosity and phase segregation reduce effective density and cause deviations from theoretical  $\mu/\rho$  predictions [14].

### 5.4 Photon Energy

Dominant interaction mechanisms shift with energy; alloy selection depends on application-specific photon spectra [4,8].

### 5.5 Geometry

Buildup effects become significant in thick or broad-beam configurations and require Monte-Carlo modeling [10–12].

## 6. Applications

Gamma-shielding alloys serve critical roles in nuclear power, medical imaging, aerospace systems, industrial radiography, and accelerator environments...

### 6.1 Nuclear Power

Stainless steels, Inconel superalloys, and W-containing HEAs are used in coolant channels, reactor cores, and control systems [15–16].

### 6.2 Medical Radiation Protection

Pb–Bi alloys, W-based alloys, and stainless steel components are used in radiotherapy, CT/PET systems, and radiation barriers [13–15].

### 6.3 Aerospace and Space Applications

High-strength HEAs and lightweight W-reinforced alloys provide shielding against cosmic rays and solar particle events [17–18].

### 6.4 Industrial Radiography

W–Ni–Fe alloys and Pb-based composites are used in collimators, source containers, and shielding casks [5].

### 6.5 Particle Accelerators

High-flux environments use Inconel, W-based alloys, and HEAs due to thermal stability and structural strength [16–18].

## 7. Future Directions and Conclusion

Future research directions include high-energy attenuation datasets, standardization of experimental protocols, microstructural modeling, ML-driven alloy discovery, and integrated photon–neutron shielding assessments...

### 7.1 Future Directions

- More high-energy (>10 MeV) attenuation data is needed for fusion and accelerator applications [1,13].
- Standardization of attenuation measurement protocols would improve reproducibility.
- Microstructural modeling—including porosity and phase clustering—must be coupled with Monte-Carlo simulations [17].
- Photon–neutron coupled shielding models will benefit reactor design [10–12].
- Machine-learning approaches can accelerate alloy discovery [18–20].

### 7.2 Conclusion

Gamma-ray interaction studies reveal that heavy-metal alloys and advanced HEAs offer outstanding attenuation across wide photon-energy ranges. Experimental and computational analyses consistently show strong agreement, confirming the reliability of mixture-rule and Monte-Carlo-based modeling. Remaining research gaps—such as microstructural modeling and high-energy datasets—must be addressed to enable next-generation shielding alloys for nuclear, aerospace, medical, and industrial environments.

## References

- [1] Algethami M., *Materials* 15 (2022) 2464.
- [2] Bagheri R., Ranjbar H., *Scientific Reports* 15 (2025) 12853.
- [3] Isazadeh F. et al., *Scientific Reports* (2025).

- [4] Mansy M.S., Radiation Physics and Chemistry 180 (2021) 109412.
- [5] Sayyed M.I. et al., Applied Sciences 10 (2020) 7680.
- [6] Büyükyıldız M., Journal of Nuclear Materials (2024).
- [7] Niksarlıoğlu S., Radiation Measurements 170 (2024) 107266.
- [8] Şimşek T., Journal of Alloys and Compounds (2023).
- [9] Wróbel J.S., SSRN Preprint (2024).
- [10] MCNP6 User Manual, Los Alamos National Laboratory (2020).
- [11] Geant4 Collaboration, Nuclear Instruments and Methods in Physics Research A (2023).
- [12] XMuDat Database, International Atomic Energy Agency (2024).
- [13] Abdelmonem A., Radiation Effects and Defects in Solids 179 (2024) 662.
- [14] Khan M., Metals (2024).
- [15] Sharma B., Applied Radiation and Isotopes (2023).
- [16] Thomas P., Fusion Engineering and Design (2025).
- [17] Wei L., Journal of Applied Physics (2024).
- [18] Farooq U., Radiation Physics and Chemistry (2025).
- [19] Zhang F., Journal of Materials Science (2023).
- [20] IAEA Photon Cross-Section Database (XCOM/XMuDat), IAEA (2024).